Pyramidal neurodegeneration is linked to select cytoarchitecture and cognitive impairment in behavioral variant frontotemporal dementia with tau or TDP-43 pathology

Ohm, DT[1,2], Bahena, A[1,2], Arezoumandan, S[1,2], Cousins, AQK[2], Phillips, J[2], Capp, N[1,2], Trotman, W[1,2], Xie, E[1,2], Wolk, D[3,4], McMillan, C[2], Trojanowski, JQ[5,6], Lee, EB[4,5,6], Grossman, M[2,7], Irwin, DJ[1,2,7]

1: University of Pennsylvania (Penn) Digital Neuropathology Lab, 2: Penn Frontotemporal Degeneration Center, 3: Penn Memory Center, 4: Penn Alzheimer's Disease Research Center, 5: Penn Center for Neurodegenerative Disease Research, 6: Penn Department of Pathology and Laboratory Medicine, 7: Penn Department of Neurology, Perelman School of Medicine

Penn Frontotemporal Degeneration Center

Penn Digital Neuropathology Laboratory

INTRODUCTION

- Behavioral variant frontotemporal dementia (bvFTD) is a clinical syndrome associated with two main types of proteinopathy (i.e., tau [bvFTD-tau] or TDP-43 [bvFTD-TDP]) and heterogeneous symptoms including impairments in social cognition and executive function largely mediated by frontal cortices[1].
- Comparative pathology studies in FTD find that TDP-43 pathology preferentially accumulates in ventromedial frontal cortices and upper cortical layers whereas tau pathology preferentially accumulates in dorsolateral frontal cortices and lower cortical layers[2,3].
- Comparative neurodegeneration studies are limited but suggest that bvFTD-tau and bvFTD-TDP have similar vulnerabilities to lower layer projection neuron loss in agranular frontal cortices (≤5 cortical layers)[4,5].
- Distributions of projection neurons including pyramidal neurons vary across frontal regions with dysgranular and granular cytoarchitecture (>5 layers)[6], but their vulnerability to degeneration remain poorly understood in bvFTD.
- Here, we tested the hypothesis that pyramidal neurodegeneration is greater in bvFTD-tau vs bvFTD-TDP and related to bvFTD-related cognitive deficits.

METHODS

Table 1: Participant demographics and pathologic characteristics.

Main Group *(N)*	Sex *(N)*	Education (years)	Age at death (years)	Disease Duration (years)	Post-mortem Interval (hours)	Mutation *(N)*	Primary Neuro-pathologic Diagnoses *(N)*	AD Neuro-pathologic Change *(N)*
HC *33*	F *16*	Unknown	66	N/A	16	None *0*	None *0*	Not *22*
	M *17*		[56-83]	N/A	[3-36]			Low *11*
								Int./High *0*
TDP *49*	F *24*	16	66	6	12	*C9orf72* *18*	TDP-A *21*	Not *11*
	M *25*	[10-22]	[41-96]	[1-15]	[2-30]	*GBE1* *1*	TDP-B *16*	Low *18*
						GRN *8*	TDP-C *6*	Int. *5*
						TBK1 *1*	TDP-E *6*	High *2*
tau *28*	F *9*	16	64	8	10	*MAPT* *6*	CBD *5*	Not *17*
	M *19*	[12-20]	[31-92]	[3-15]	[3-41]		PiD *12*	Low *9*
							PSP *5*	Int. *0*
							TauU *6*	High *1*

HC=healthy unimpaired control; F=female; M=male; *MAPT*=microtubule-associated protein tau on chromosome 17; *C9orf72*=short (p) arm of chromosome 9 open reading frame 72; *GBE*=glycogen branching enzyme; *GRN*=granulin; *TBK1*=TANK-binding kinase 1; AD=Alzheimer disease, CBD=corticobasal degeneration, PiD=Pick disease, PSP=progressive supranuclear palsy, TauU=unclassifiable tauopathy. Non-italicized numbers are medians, brackets enclose ranges.

- Paraffin-embedded 6µm-thick tissue from anterior cingulate (aCC), medial orbitofrontal (OFC), and middle frontal cortex (MFC) were immunostained using antibodies to tau (AT8), TDP-43 (1D3), neuronal nuclear protein found in most neurons (NeuN), and non-phosphorylated neurofilament enriched in pyramidal neurons (SMI32). All tissue was counterstained with hematoxylin.
- In up to 5 aCC subregions, 5 mOFC subregions, and 1 MFC subregion spanning six Brodmann areas [BA] (i.e., 33, 24, 32, 14, 11, 46) per brain, we used a belt-transect method to sample cortical layers ~1 mm-wide (**Fig. 1**).
- We digitally quantified the percent area occupied (%AO) by immunoreactivites in supragranular (II-III) layers, infragranular (V-VI) layers, and all layers combined using automated thresholding methods validated with visual ratings.
- Supragranular predominance of SMI32 defined distinct cytoarchitectonic areas[6]:

$$\textbf{\% supragranular} = \frac{[\text{supragranular SMI32 \%AO}]}{[\text{supragranular SMI32 \%AO} + \text{infragranular SMI32 \%AO}]} \; X\,100$$

where larger % represents more supragranular-predominant "externopyramidal" areas (**Fig. 1C**)

- Natural log (ln) transformation normalized %AO data used in linear mixed-effect models adjusted for region, hemisphere, fixative, age, and postmortem interval performed in SPSS (v28) (**Fig. 1-3**). Multiple comparisons were Bonferroni corrected (**Fig. 2**). Exploratory analyses compared SMI32 to letter fluency (an executive functioning test) available <5 years from symptom onset (n=23) (**Fig. 3**).

RESULTS

Figure 1. Anatomical gradients in cytoarchitecture predict divergent patterns of neurodegeneration in bvFTD-tau vs bvFTD-TDP.

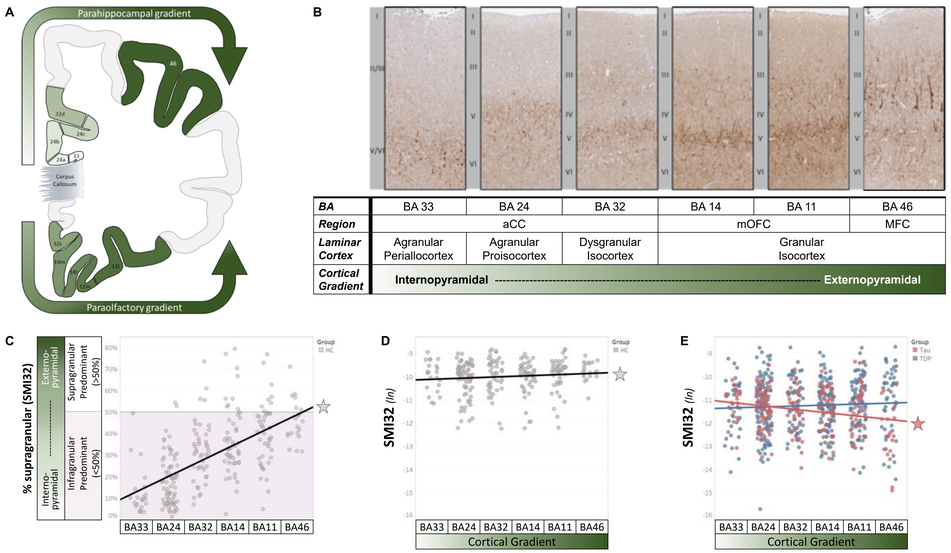

1A) Anatomical model of cortical subregions sampled and the cytoarchitectonic gradients they form in the frontal lobe. *Cortices colored gray were not included in study.* **1B-C)** Photomicrographs and laminar measures show SMI32 supragranular predominance increases along regions arranged medial-to-lateral (β=0.07,SE=0.005,p<0.001)*. **1D)** SMI32 in layers combined modestly increases along the cortical gradient in HC (β=0.07,SE=0.02,p<0.001)*. **1E)** In contrast, the cortical gradient is not associated with SMI32 loss in bvFTD-TDP (p>0.05) and is negatively associated with SMI32 loss in bvFTD-tau (β=-0.12,SE=0.03,p<0.001)*.

Figure 2. SMI32 loss reflects region-specific pyramidal neurodegeneration in bvFTD-tau vs bvFTD-TDP.

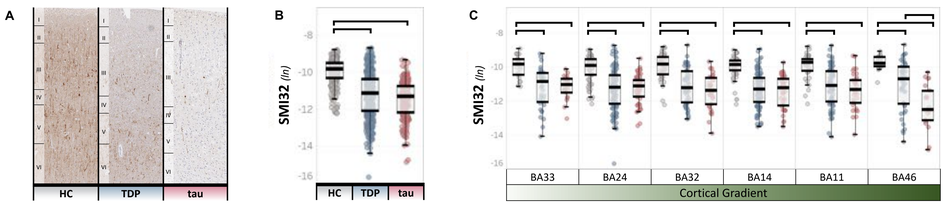

2A) Representative laminar distributions of SMI32 in the MFC of each group. **2B)** While SMI32 is reduced in bvFTD-TDP (p<0.001) and bvFTD-tau (p<0.001) compared to HC, SMI32 is not different between bvFTD groups (p>0.05). Overall neurodegeneration (NeuN data not shown) show similar patterns. **2C)** Analyses by region show similar patterns except in BA46 (MFC) which shows greater SMI32 loss in bvFTD-tau compared to both HC (p<0.001) and bvFTD-TDP (p=0.006).

Figure 3. Early executive dysfunction is related to pyramidal neurodegeneration in bvFTD.

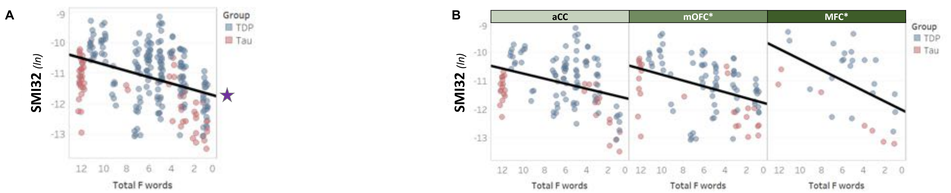

3A) Early executive dysfunction (i.e., fewer F words) is associated with greater SMI32 loss in regions and groups combined (β=0.12,SE=0.04,p=0.015)*. **3B)** Analyses by region indicate executive dysfunction is related to SMI32 loss in mOFC (β=0.11,SE=0.05,p=0.034)* and MFC (β=0.09,SE=0.04,p=0.045)*, not aCC (p>0.05).

Figure 4. Regional distributions of pyramidal neurodegeneration and pathologic burden in bvFTD-TDP vs bvFTD-tau.

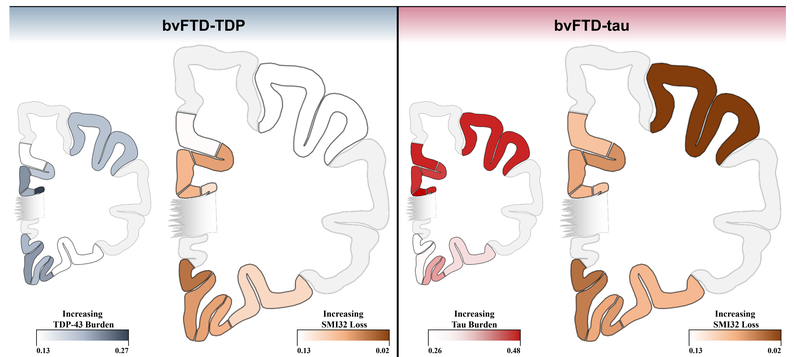

In bvFTD-TDP, peak pyramidal neurodegeneration (SMI32 loss) and TDP-43 pathologic burden overlap in more medial, internopyramidal areas including perigenual cingulate regions.

In bvFTD-tau, peak pyramidal neurodegeneration (SMI32 loss) and tau pathologic burden overlap in more dorsal regions, especially the externopyramidal areas of MFC.

Because absolute %AO data varied by pathologic subgroups, all data were scaled to a comparable 0-1 range reflecting increasing severity using min-max normalization within each pathologic subgroup for each marker of interest (i.e., AT8, 1D3, SMI32).

MAIN FINDINGS & CONCLUSIONS

- ❖ Anatomical gradients intrinsic to frontal lobes (**Fig. 1A-D**) predict increasing severity of pyramidal neurodegeneration in bvFTD-tau, not bvFTD-TDP (**Fig. 1E**).
- ❖ Furthermore, we find greater pyramidal neurodegeneration in the externopyramidal area of middle frontal cortex of bvFTD-tau vs bvFTD-TDP and HC (**Fig. 2A,C**).
- ❖ Lastly, pyramidal neurodegeneration may contribute to executive dysfunction in bvFTD, especially in more externopyramidal areas (i.e., orbitofrontal, middle frontal cortex) (**Fig. 3A,B**).
- ❖ Our results suggest that while pyramidal loss is a common feature in select frontal areas and likely contributes to cognitive impairment in bvFTD, distinct cytoarchitectonic areas may preferentially influence tau-mediated degeneration of pyramidal neurons (**Fig. 4**).
- ❖ Future work will investigate additional cell types in larger region and cortical layer analyses to identify disease-specific mechanisms of vulnerability and spread that may inform new neuroprotective therapeutic targets.

REFERENCES

1. Cairns, N.J. *et al.* Neuropathologic diagnostic and nosologic criteria for frontotemporal lobar degeneration: consensus of the Consortium for Frontotemporal Lobar Degeneration. *Acta Neuropathol* **114** 5–22 (2007).
2. Ohm, D.T. *et al.* Signature laminar distributions of pathology in frontotemporal lobar degeneration. *Acta Neuropathol* **143**, 363–382 (2022).
3. Giannini, L.A.A. *et al.* Frontotemporal lobar degeneration proteinopathies have disparate microscopic patterns of white and grey matter pathology. *Acta Neuropathologica Commun* **9**, 30 (2021).
4. Lin, L.-C. *et al.* Preferential tau aggregation in von Economo neurons and fork cells in frontotemporal lobar degeneration with specific MAPT variants. *Acta Neuropathol Comm* **7**, 159 (2019).
5. Nana, A.L. *et al.* Neurons selectively targeted in frontotemporal dementia reveal early stage TDP-43 pathobiology. *Acta Neuropathol* **137**, 27–46 (2019).
6. García-Cabezas M.Á., *et al.* A Protocol for Cortical Type Analysis of the Human Neocortex Applied on Histological Samples, the Atlas of Von Economo and Koskinas, and Magnetic Resonance Imaging. *Front Neuroanat* **14**, 576015 (2020).

ACKNOWLEDGMENTS

NIH grants NINDS R01-NS109260-01A1, NIA P01-AG066597, NIA P30-AG072979, NIA U01-AG052943-01, NIA K01-AG-081484-01, Penn Institute on Aging, DeCrane Family foundation.

We thank the patients and families for their generous commitment to research and invaluable gift of brain donation to make this work possible. We extend our gratitude and remembrance to Drs. Murray Grossman and John Trojanowski whose legacies in FTD research are far reaching and deeply impactful.

Contact Information:
Daniel.ohm@pennmedicine.upenn.edu